Metal–Ion Chelation

DOI: 10.1002/anie.200906601

Single-Molecule Kinetics of Two-Step Divalent Cation Chelation**

*Anne F. Hammerstein, Seong-Ho Shin, and Hagan Bayley**

Despite the importance of divalent metal–ion chelators in numerous areas, including basic biology[1] and medicine,[2–4] our understanding of the thermodynamic basis of chelation[5,6] and the kinetics of metal–ion binding and dissociation is far from complete. Ensemble techniques, such as NMR lineshape analysis, have been used to investigate the kinetics of various chelators with many divalent cations.[7–11] However, there have been complications with these approaches. For example, a chelator such as EDTA can promote the exchange of a metal ion from a preformed [M·EDTA] complex. Further, metal complexes can undergo protonation and proton transfer can be rate determining in metal–ion exchange, and exchange rates can vary depending on the presence of monovalent cations, for example, Na^+ versus K^+. These factors have lead to the postulation of complex reaction mechanisms for metal chelation with numerous rate constants that must often be reconciled with a relative paucity of data.

Single-molecule methods should be capable of shedding light on complex multistep processes, including chelation. By using a protein nanoreactor,[12] we were able to monitor the association and dissociation of individual divalent metal ions with clusters of imidazole ligands.[13,14] Recently, single-molecule fluorescence was used to examine the formation and dissociation of a Cu^{2+} complex.[15] But, in neither case were the steps in complex formation resolved. Herein, we use the nanoreactor approach to monitor the formation of an EDTA-like complex with Zn^{2+} and obtain rate constants for the eight major steps in the reversible chelation of the cation. The approach has the potential for further untangling the intricacies of metal–ion complexation, and might also be extended to examine metal–ion catalysis and the stochastic detection of metal ions in solution.

To build a metal–ion binding site, we performed a dual-site chemical modification on cysteine residues positioned by mutagenesis within the lumen of the α-hemolysin (αHL) pore. For this purpose, we synthesized a "half-chelator" ligand, comprising the *N*-propyliminodiacetic acid (PIDA) group and an iodoacetamide group for covalent attachment to the protein (Figure 1a). We reasoned that a complex formed by two half-chelators would resemble complexes formed by EDTA. An αHL pore with a cysteine residue at position 117 had been used previously to observe covalent bond formation at the single-molecule level,[16] so we reasoned that this position would also be suitable for the observation of complex formation between a half-chelator and a divalent metal ion. Model building suggested that a second ligand on residue 143 of the same αHL subunit would be favorably positioned for full complex formation (Figure 1b,c). The monomeric polypeptides αHL T117C/G143C and αHL T117C were prepared by in vitro transcription and translation. The heteroheptameric pores P_{PIDA} (which has a single half-chelator at position 117 on one of the seven subunits) and $P_{(PIDA)2}$ (which has one half-chelator at each of positions 117 and 143 on one of the seven subunits) were prepared, by using chemically modified subunits in combination with unmodified wild-type (WT) subunits.[17]

P_{PIDA} and $P_{(PIDA)2}$ were characterized by single-channel recording in planar lipid bilayers. P_{PIDA} carried a single-channel current of (-73.8 ± 2.5) pA at -50 mV in 2 M KCl, 10 mM 3-morpholinopropane-1-sulfonic acid (MOPS), pH 7.0 (Table S1 in the Supporting Information). The addition of Zn^{2+} to the trans recording chamber resulted in the fluctuation of the ionic current between two discrete levels separated by $\Delta I = (1.6 \pm 0.1)$ pA, where ΔI is the current difference between the level partially blocked by Zn^{2+} and that of the unoccupied pore (Figure 2a). The events associated with Zn^{2+} were not seen in buffer containing 1 mM EDTA or with WT_7 pores (data not shown) and had a mean lifetime ($\tau_{off\text{-}mono7}$) of (251 ± 13) ms. In a kinetic analysis of the events, we assumed that the half-chelator and Zn^{2+} reversibly form a binary complex (Figure 2b) and that the Zn^{2+} "concentration" inside the pore equals that in solution.[12] The reciprocal of the mean inter-event interval ($\tau_{on\text{-}mono7}$) is proportional to the Zn^{2+} concentration (Figure 2c), which is consistent with a bimolecular interaction for which $1/\tau_{on\text{-}mono7} = k_{on\text{-}mono7}[Zn^{2+}]$. In contrast, a plot of the reciprocal of the mean lifetime of the complex ($\tau_{off\text{-}mono7}$) versus the Zn^{2+} concentration has a near zero slope (Figure 2c), which is consistent with a unimolecular dissociation mechanism ($1/\tau_{off\text{-}mono7} = k_{off\text{-}mono7}$). The forward and reverse rate constants derived from the τ values (Figure 2c; $k_{on\text{-}mono7} = (1.5 \pm 0.2) \times 10^5\ M^{-1}s^{-1}$, $k_{off\text{-}mono7} = (4.0 \pm 0.2)\ s^{-1}$) yield a formation constant of $K_{f\text{-}mono7} = (3.8 \pm 0.5) \times 10^4\ M^{-1}$ at 24 °C ($n = 4$ independent experiments). Formation of the half-chelator·Zn^{2+} complex is only possible when the half-chelator is in the deprotonated state,[5,18,19] the probability of which is determined by the pH value of the recording buffer (the pK_a values of *N*-methyliminodiacetic acid (MIDA) are 2.5 and 9.5).[11] Consequently, the values of both $k_{on\text{-}mono}$ and $K_{f\text{-}mono}$ depend on the pH (see the Supporting Information). As the half-chelator is tridentate, there are vacant coordination sites on the Zn^{2+} ion. These sites are likely to be occupied by water or chloride ligands, which

[*] A. F. Hammerstein, Dr. S.-H. Shin, Prof. Dr. H. Bayley
Department of Chemistry, University of Oxford
Chemistry Research Laboratory
Mansfield Road, Oxford, OX1 3TA (UK)
Fax: (+44) 1865-275-708
E-mail: hagan.bayley@chem.ox.ac.uk
Homepage: http://bayley.chem.ox.ac.uk/

[**] Supported by the MRC.

Supporting information for this article (including experimental procedures) is available on the WWW under http://dx.doi.org/10.1002/anie.200906601.

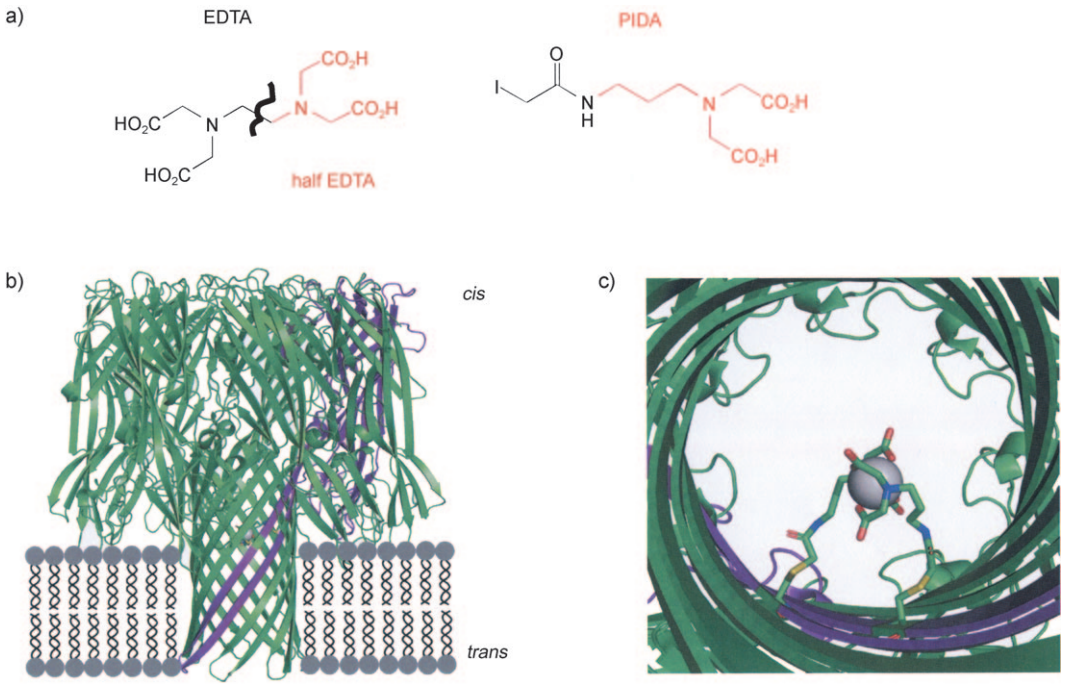

Figure 1. Dual-site modification of the αHL pore. a) Half of the hexadentate chelator EDTA (red) served as a model for the half-chelator ligand. The half-chelator reagent contains a PIDA (*N*-propyliminodiacetic acid) group (red) and an iodoacetamide group for covalent attachment to the protein. b) The P_{PIDA} and $P_{(PIDA)2}$ pores consist of six wild-type subunits (green) and one modified subunit (purple). c) View inside the β barrel of the modified $P_{(PIDA)2}$ pore. Two molecules of PIDA are connected to the protein backbone at positions 117 and 143 and form a complex with a divalent metal ion (gray sphere). EDTA = ethylendiaminetetraacetate.

typically have very fast exchange rates[20,21] and would not be observed at the time resolution of the experiments described here (≈0.3 ms). Partial dissociation and association of the half-chelator at one or two of the three coordination sites would also be undetectable in our experiments.

The $P_{(PIDA)2}$ pore had a single-channel current of (−67.0 ± 2.8) pA at −50 mV in 2 M KCL, 10 mM MOPS, pH 7.0 (Table S1 in the Supporting Information). Upon the addition of 10 μM of Zn^{2+} to the trans recording chamber, we observed very long binding events (ΔI = (3.7 ± 0.3) pA) that lasted from tens of seconds to several minutes (Figure 3a). We believe that these events represent complex formation between both half-chelators and a single Zn^{2+} ion. Because the binding events were so long, it was difficult to perform a detailed kinetic analysis. Therefore, we lowered the pH of the recording buffer from 7.0 to 4.0, thereby decreasing

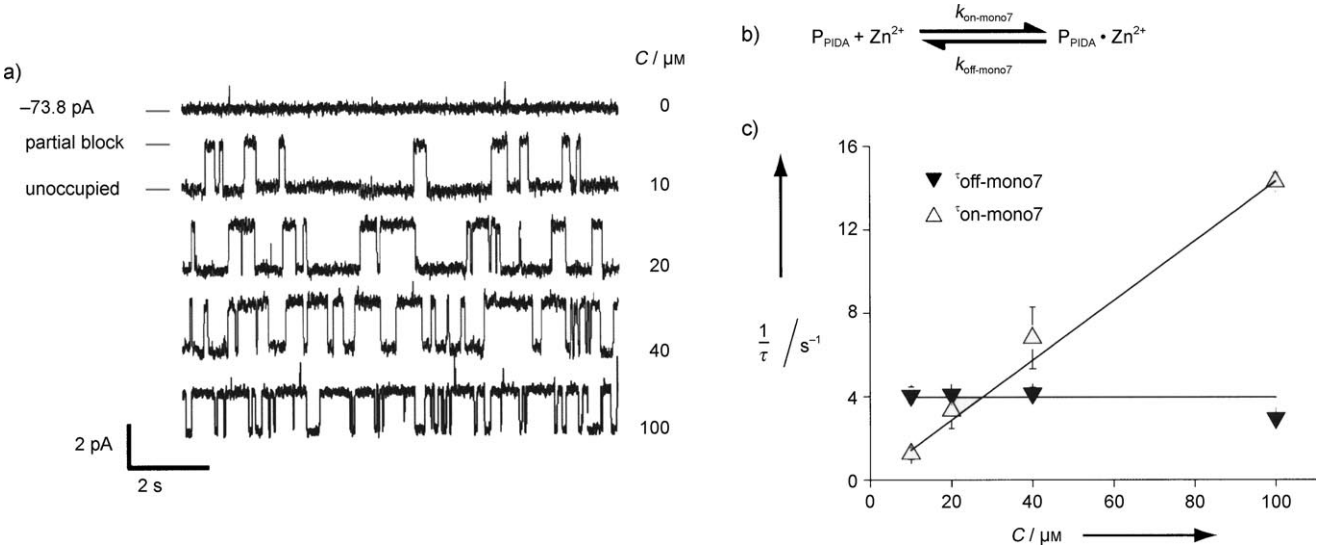

Figure 2. The P_{PIDA} pore has a single binding site for a divalent metal ion and binds Zn^{2+} reversibly. a) Single-channel recordings at −50 mV with a buffer containing 2.0 M KCl and 10 mM MOPS (pH 7.0) in both chambers, and 0 to 100 μM $ZnCl_2$ in the trans chamber. The two current levels of the P_{PIDA} pore correspond to the unoccupied pore and to the partial block caused by Zn^{2+} binding to the half-chelator in the pore. b) Proposed kinetic scheme describing Zn^{2+} binding to the P_{PIDA} pore. c) Reciprocals of the mean inter-event intervals ($\tau_{on\text{-}mono7}$; △) and the dwell times of Zn^{2+} ($\tau_{off\text{-}mono7}$; ▼) versus the Zn^{2+} concentration. The values of $\tau_{on\text{-}mono7}$ and $\tau_{off\text{-}mono7}$ were determined by fitting dwell-time histograms for each Zn^{2+} concentration to single exponential functions. For a simple bimolecular interaction: $k_{off} = 1/\tau_{off}$ and $k_{on} = 1/\tau_{on}$ [Zn^{2+}]. MOPS = 3-(*N*-morpholine)-propanesulfonic acid.

the amount of time the half-chelators spend in the active deprotonated state (see the Supporting Information).

At pH 4.0, various Zn^{2+} binding events were observed with $P_{(PIDA)2}$ (Figure 3b). Rare short binding events resulted in two distinct partially blocked current levels: level A ($\Delta I = (1.9 \pm 0.04)$ pA) and level B ($\Delta I = (2.5 \pm 0.2)$ pA). By comparison, Zn^{2+} binding events in the P_{PIDA} pore, at pH 4.0, had a single ΔI value of (1.6 ± 0.03) pA (data not shown). We interpret the short binding events in the $P_{(PIDA)2}$ pore to correspond to the two possible complexes between a Zn^{2+} ion and one or the other of the half-chelators at positions 117 and 143. The two different ΔI values for the block must result from the slightly different environments of the half-chelators inside the β barrel, a phenomenon that is also seen with cysteine–arsenic(III) adducts.[22]

With the $P_{(PIDA)2}$ pore, at pH 4.0, long Zn^{2+} binding events were also seen, which comprised three different current levels. The long events always began as a step from the unoccupied pore level to either level A or level B (i.e. complex formation by one half-chelator), followed by a step to a new current level, C. As supported by subsequent findings, level C represents the full chelator·Zn^{2+} complex formed by the participation of both half-chelators. From level C, current steps to level A or B were observed, but we never detected steps directly to the level of the unoccupied pore. Therefore, the association of Zn^{2+} to form the full chelator complex is a process with two major steps, featuring an intermediate state (A or B) in which the metal ion is complexed by only one half-chelator (Figure 3c). Again, substeps involving the dissociation or association of one or

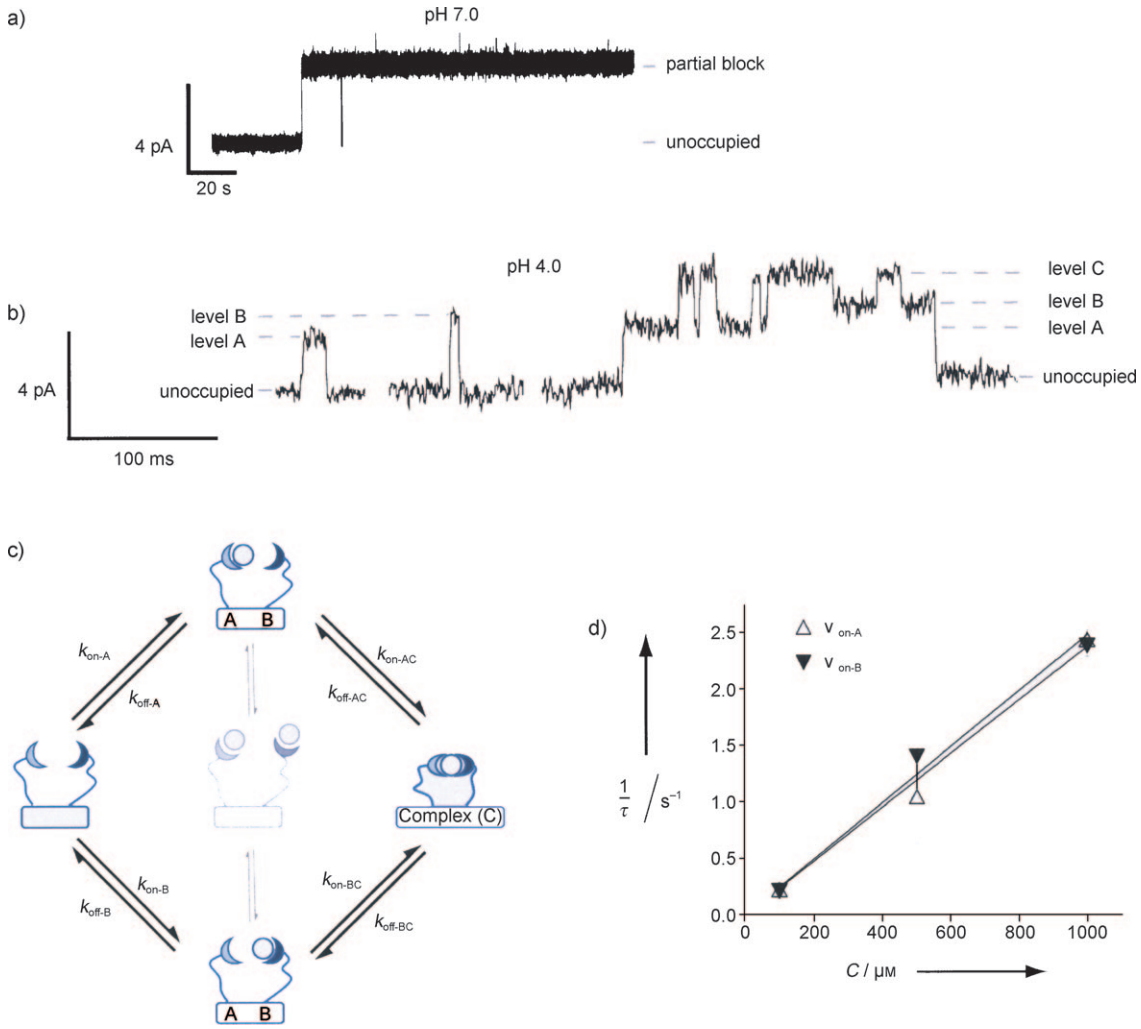

Figure 3. Binding of Zn^{2+} to the $P_{(PIDA)2}$ pore. a) Single-channel recording at −50 mV with a buffer containing 2.0 M KCl and 10 mM MOPS (pH 7.0) in both chambers, and 10 μM Zn^{2+} in the trans chamber. The Zn^{2+} binding events were very long, lasting from tens of seconds to several minutes. b) Complex formation at pH 4.0 proceeds through intermediate steps. Single-channel recording at −50 mV with a buffer containing 2.0 M KCl and 10 mM potassium acetate (pH 4.0) in both chambers, and 1 mM $ZnCl_2$ in the trans chamber. The four different current levels correspond to the unoccupied pore, a single Zn^{2+} ion bound to one or the other of the half-chelators (levels A and B), and the Zn^{2+} ion bound to both chelators (level C). Sub-steps during the association and dissociation of each tridentate half-chelator are not observed. c) Proposed kinetic scheme describing the formation of the complex at pH 4.0. d) The Zn^{2+} concentration dependence of the reaction rates for chelation sites A ($v_{on\text{-}A}$, ▼) and B ($v_{on\text{-}B}$, △).

two of the three coordinating sites of a half-chelator are too fast to be detected.

The reaction rates in the binding scheme for Zn^{2+} by the $P_{(PIDA)2}$ pore (Figure 3c and Scheme S3 in the Supporting Information) were determined by fitting the lifetimes of the four different states (unoccupied, A, B, C) to the scheme by using the QuB software package (Table 1 and Figure S4 in the Supporting Information). Plots of the reaction rates $v_{A\text{-}on}$ and $v_{B\text{-}on}$ at pH 4.0, (s^{-1}, from QuB), versus the Zn^{2+} concentration (Figure 3d) are of the form $v = k[Zn^{2+}]$, where k is $k_{on\text{-}A4}$ or $k_{on\text{-}B4}$ ($M^{-1}s^{-1}$), which confirms that the formation of both half-chelator·Zn^{2+} complexes involves a bimolecular reaction. In contrast, the rates of formation of C from A and B, are independent of the concentration of Zn^{2+} (Figure S5 in the Supporting Information), confirming that C contains a single Zn^{2+} ion, that is, the two half-chelators are not simultaneously occupied at pH 4.0, each by one Zn^{2+} ion ("transparent" state, Figure 3c). As a further test of the kinetic scheme, we note that at equilibrium, the product of the rate constants for a clockwise movement around the diamond in Figure 3c must equal the product for the anticlockwise movement.[23] We found that $k_{on\text{-}A4}k_{on\text{-}AC4}k_{off\text{-}BC4}k_{off\text{-}B4} = (96 \pm 25) \times 10^6\,M^{-1}s^{-4}$ and $k_{on\text{-}B4}k_{on\text{-}BC4}k_{off\text{-}AC4}k_{off\text{-}A4} = (113 \pm 22) \times 10^6\,M^{-1}s^{-4}$, which are equal within experimental error. The rate constants in Table 1 yield the formation constants $K_{f\text{-}A4} = (92 \pm 15)\,M^{-1}$ and $K_{f\text{-}B4} = (102 \pm 13)\,M^{-1}$ for the half-chelator(A)·Zn^{2+} and half-chelator(B)·Zn^{2+} complexes respectively, and $K_{f(C\ via\ A)4} = (147 \pm 26)\,M^{-1}$ and $K_{f(C\ via\ B)4} = (163 \pm 37)\,M^{-1}$ for the formation of the full chelator·Zn^{2+} complex. The latter values should be and are equal ($K_{f\text{-}C4}$) within experimental error.

Table 1: Kinetic constants for the formation of complexes between the $P_{(PIDA)2}$ pore and Zn^{2+} at pH 4.0.[a]

	Level A	Level B	Level C (via A)	Level C (via B)
k_{on}	$k_{on\text{-}A4}$ (2490±370) $M^{-1}s^{-1}$	$k_{on\text{-}B4}$ (2340±60) $M^{-1}s^{-1}$	$k_{on\text{-}AC4}$ (51±5) s^{-1}	$k_{on\text{-}BC4}$ (56±7) s^{-1}
k_{off}	$k_{off\text{-}A4}$ (27±2) s^{-1}	$k_{off\text{-}B4}$ (23±3) s^{-1}	$k_{off\text{-}AC4}$ (32±4) s^{-1}	$k_{off\text{-}BC4}$ (35±5) s^{-1}
K_f	$K_{f\text{-}A4}$ (92±15) M^{-1}	$K_{f\text{-}B4}$ (102±13) M^{-1}	$K_{f(C\ via\ A)4}$ (147±26) M^{-1}	$K_{f(C\ via\ B)4}$ (163±37) M^{-1}

[a] The kinetic constants were obtained by using the QuB software package. Formation constants (K_f) were calculated by using $K_f = k_{on}/k_{off}$.

The relationship between the first and second affinity constants for a chelator can be thought of in terms of the effective molarity of the second half-chelator. The effective molarity (M_{eff}) is an empirical term that relates the kinetics and equilibria of intramolecular and intermolecular reactions (Scheme 1).[24,25]

In the present case, M_{eff} is the concentration of PIDA that theoretically would be present in solution to obtain the same extent of full chelation of Zn^{2+} as observed in the intramolecular case. The M_{eff} value depends on the length and flexibility of the linker between the two half-chelators[24] and reflects the proximity of the two reactive groups (i.e. the second half-chelator and the metal ion) and whether they have the correct orientation for complex formation.[26,27] In our calculations, we assume that $K_f^{intra} = K_{f\text{-}AC4}$ and that $K_f^{inter} = K_{f\text{-}A4}$, thus giving $M_{eff} = 17$ mM. The use of $K_{f\text{-}B4}$ and $K_{f\text{-}BC4}$ gives a similar result. Our calculations are likely to overestimate K_f^{inter}, because successive formation constants for Zn^{2+}·amino acid complexes tend to decrease.[28] The value of 17 mM therefore represents a minimum estimate of M_{eff}. M_{eff} values of the same order of magnitude were obtained for the intramolecular binding of a ligand covalently attached to the surface of a protein[24] and for the bivalent binding of porphyrins to N-methylimidazole-functionalized gold nanoparticles.[29]

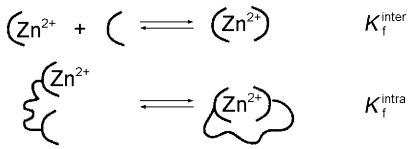

Scheme 1. $M_{eff} = K_f^{intra}/K_f^{inter}$ (K_f^{inter} is expressed in units of M, while K_f^{intra} is dimensionless).

The same value of M_{eff} should be applicable at all pH values. Therefore, with M_{eff} in hand, we can reconsider Zn^{2+} binding at pH 7.0, for which we found $k_{on\text{-}mono7} = 1.5 \times 10^5\,M^{-1}s^{-1}$, $k_{off\text{-}mono7} = 4.0\,s^{-1}$ and $K_{f\text{-}mono7} = 3.8 \times 10^4\,M^{-1}$ for P_{PIDA}, the pore containing a single half-chelator. The $k_{on\text{-}mono7}$ value is 60 times higher than $k_{on\text{-}A4}$, a finding which is not surprising as the deprotonated half-chelator ($pK_a \approx 9.5$) is expected to bind more rapidly than the protonated form. Also, the $k_{off\text{-}mono7}$ value is 6.8 times lower than $k_{off\text{-}A4}$. The origin of this decrease in rate is less obvious, although the half-chelator must must undergo reprotonation during one of the (invisible) sub-steps involved in dissociation. By using $M_{eff} = K_f^{intra}/K_f^{inter}$, and putting $K_f^{inter} = K_{f\text{-}mono7}$, we find $K_f^{intra} = 646$ ($= K_{f\text{-}AC7}$, or $K_{f\text{-}BC7}$), which is far greater in comparison with the value of 1.6 for $K_{f\text{-}AC4}$ (at pH 4.0). The overall affinity constant at pH 7.0 is then $K_{f\text{-}C7} = K_{f\text{-}mono7} \cdot K_f^{intra} = 2.5 \times 10^7\,M^{-1}$ (Table 2), which indicates an increase of more than five logarithmic units compared to the value at pH 4.0. The

Table 2: Kinetic constants for the formation of complexes between the P_{PIDA} pore and Zn^{2+} and estimated kinetic constants for the $P_{(PIDA)2}$ pore at pH 7.0.[a]

	Level A[b]	Level C (via A)
k_{on}	$k_{on\text{-}mono7}$ $(1.5 \pm 0.2) \times 10^5\,M^{-1}s^{-1}$	$k_{on\text{-}AC7}$ 2550 s^{-1}
k_{off}	$k_{off\text{-}mono7}$ (4.0±0.2) s^{-1}	$k_{off\text{-}AC7}$[c] 4.0 s^{-1}
K_f	$K_{f\text{-}mono7}$ $(3.8 \pm 0.5) \times 10^4\,M^{-1}$	$K_{f\text{-}C7}$[c] $2.5 \times 10^7\,M^{-1}$

[a] The kinetic constants for P_{PIDA} were obtained as described in the text. $k_{on\text{-}AC7}$ and $K_{f\text{-}C7}$ for $P_{(PIDA)2}$ were estimated by using $M_{eff} = 17$ mM and the values for $k_{on\text{-}mono7}$ and $K_{f\text{-}mono7}$ for P_{PIDA}. [b] Because ΔI for the Zn^{2+} block of the P_{PIDA} pore is similar to ΔI for level A in the $P_{(PIDA)2}$ pore, it is likely, but not certain, that level A represents Zn^{2+} binding to the half-chelator at position 117. [c] The estimates for $P_{(PIDA)2}$ tacitly assume that the k_{off} values for the two steps in chelation by $P_{(PIDA)2}$ are the same at a given pH, which is not quite true (e.g. $k_{off\text{-}A}$ and $k_{off\text{-}AC}$, Table 1).

partitioning of the intermediate A (or B) between the fully chelated form C and the form with double Zn^{2+} occupancy (Figure 3c) will be in the ratio $M_{eff}/[Zn^{2+}]$ to 1. Therefore, double occupancy will only be observed at very high concentrations of Zn^{2+}, and we indeed found no evidence for this species. The value of $K_{f\text{-}mono7}$ and $K_{f\text{-}AC7}$ are lower than the values for binding a first and a second MIDA molecule in solution,[11] but the literature values are based on fully deprotonated MIDA ($pK_a = 9.5$) and the value for the second MIDA is expressed in units of M^{-1}.

These estimates of the rate constants make sense in the light of additional observations at pH 7.0. First, we see only a single step upon Zn^{2+} binding (Figure 3a). Because $k_{on\text{-}AC7} \approx 2550\ s^{-1}$ ($M_{eff}\,k_{on\text{-}mono7}$), the mean lifetime of the intermediate with one occupied half-chelator is $\tau_{on\text{-}AC7} = 1/k_{on\text{-}AC7} \approx 390\ \mu s$, which would be difficult to observe under our recording conditions. Second, the overall dwell time of Zn^{2+} at the binding site in $P_{(PIDA)2}$ in all states (A, B, and C) is given by $\tau_{ABC} \approx (1/k_{off\text{-}A})(1+k_{on\text{-}AC}/2\,k_{off\text{-}AC})$.[30] A statistical factor of two is applied because there are two pathways for dissociation of the fully chelated Zn^{2+} (complex C). At pH 7.0, this equation predicts $\tau_{ABC} = 80$ s. Knowing this, we performed additional measurements at pH 7.0 and found that $\tau_{ABC} =$ 193 s (95% confidence interval 130, 316 s, $n = 20$ events), which is in reasonable agreement given the assumptions made in the calculation (Table 2).

Although it is difficult to make a detailed comparison because few rate contants have been measured directly in ensemble experiments, the rate constants that have been determined here are consistent with those found in the literature. For example, a value of $50\ s^{-1}$ was determined by NMR line-shape analysis for $[Zn(MIDA)_2{}^{2-}] \rightarrow [ZnMIDA] + MIDA^{2-}$.[11] Furthermore, the exchange rate was independent of the pH value over the range 6.0 to 9.0. By comparison, we determined a rate constant of $\approx 35\ s^{-1}$ at pH 4.0 for the dissociation of the second PIDA ligand in our system (Table 1). We also found that the dissociation rate for the first PIDA lacked a strong dependence on pH: at pH 7.0, $k = 4\ s^{-1}$; while at pH 4.0, $k \approx 25\ s^{-1}$ (Table 1 and Table 2). The affinities of $P_{(PIDA)2}$ for Zn^{2+} are lower than those in the literature for EDTA ($\log K_f = 16.5$),[28] although as Toone and co-workers have indicated,[5] it is difficult to find data that can be compared given the effects of buffer ions and the need for rigorous control over the pH during titration experiments. Furthermore, in our case, Zn^{2+} is binding against a voltage gradient, which can also alter the rate constants.[12] It is also clear that small structural changes can dramatically alter the affinity of chelators. For example, the affinity of Ca^{2+} for PDTA (1,3-diaminopropanetetracetic acid), with one additional methylene unit between the two nitrogen atoms, is 10^4 times lower than that of EDTA.[5] Given the additional conformational freedom of the two PIDA groups in $P_{(PIDA)2}$ compared with the two arms of EDTA, which must produce unfavorable entropic contributions as well as decreased relief from unfavorable electrostatic interactions in the binding of Zn^{2+},[5] it is hardly surprising that the affinity of $P_{(PIDA)2}$ is respectable, but not exceptionally strong.

In this study, we have been able to monitor complex formation between an engineered chelator and a divalent metal ion in real time, thereby establishing a new means to obtain kinetic and thermodynamic data for the formation of metal–ion complexes. For example, we revealed the principal intermediates in complex formation between two half-chelators and a Zn^{2+} ion and determined all the major rate constants involved in this process. Such detail, which is normally lost in ensemble measurements, highlights the wealth of additional chemical information available from a single-molecule approach. Furthermore, several of the potential complexities of ensemble experiments cannot occur in the single-molecule format and others can be ruled out. For example, there is no excess chelator able to promote divalent cation exchange, and we saw no evidence for the additional states that might indicate exchange mediated by slow proton transfer.[9,10] In addition to our enhanced ability to obtain information about the chelation of metal ions, we envision that the divalent metal ion complexes that we have formed inside the β barrel of the αHL pore will be useful for investigating metal–ion catalysis in aqueous solution[31–33] at the single-molecule level, and for developing improved means for the stochastic detection of metal ions.[13,14,34]

Received: November 23, 2009
Revised: April 20, 2010
Published online: June 22, 2010

Keywords: chelating ligands · kinetics · nanoreactors · single-molecule studies

[1] R. M. Paredes, J. C. Etzler, L. T. Watts, W. Zheng, J. D. Lechleiter, *Methods* **2008**, *46*, 143.
[2] D. S. Kalinowski, D. R. Richardson, *Pharmacol. Rev.* **2005**, *57*, 547.
[3] K. Tanaka, K. Fukase, *Org. Biomol. Chem.* **2008**, *6*, 815.
[4] M. D. Cappellini, P. Pattoneri, *Annu. Rev. Med.* **2009**, *60*, 25.
[5] T. Christensen, D. M. Gooden, J. E. Kung, E. J. Toone, *J. Am. Chem. Soc.* **2003**, *125*, 7357.
[6] A. D. Hughes, E. V. Anslyn, *Proc. Natl. Acad. Sci. USA* **2007**, *104*, 6538.
[7] D. W. Margerum, D. L. Janes, H. M. Rosen, *J. Am. Chem. Soc.* **1965**, *87*, 4463.
[8] R. J. Kula, G. H. Reed, *Anal. Chem.* **1966**, *38*, 697.
[9] D. L. Rabenstein, R. J. Kula, *J. Am. Chem. Soc.* **1969**, *91*, 2492.
[10] R. G. Pearson, D. G. Dewit, *J. Coord. Chem.* **1973**, *2*, 175.
[11] P. Mirti, M. C. Gennari, *J. Inorg. Nucl. Chem.* **1977**, *39*, 1259.
[12] H. Bayley, T. Luchian, S.-H. Shin, M. B. Steffensen in *Single Molecules and Nanotechnology* (Eds.: R. Rigler, H. Vogel), Springer, Heidelberg, **2008**, p. 251.
[13] O. Braha, B. Walker, S. Cheley, J. J. Kasianowicz, L. Song, J. E. Gouaux, H. Bayley, *Chem. Biol.* **1997**, *4*, 497.
[14] O. Braha, L.-Q. Gu, L. Zhou, X. Lu, S. Cheley, H. Bayley, *Nat. Biotechnol.* **2000**, *18*, 1005.
[15] A. Kiel, J. Kovacs, A. Mokhir, R. Kramer, D. P. Herten, *Angew. Chem.* **2007**, *119*, 3427; *Angew. Chem. Int. Ed.* **2007**, *46*, 3363.
[16] S.-H. Shin, T. Luchian, S. Cheley, O. Braha, H. Bayley, *Angew. Chem.* **2002**, *114*, 3859; *Angew. Chem. Int. Ed.* **2002**, *41*, 3707.
[17] S. Loudwig, H. Bayley, *J. Am. Chem. Soc.* **2006**, *128*, 12404.
[18] R. Y. Tsien, *Biochemistry* **1980**, *19*, 2396.
[19] C. Patton, S. Thompson, D. Epel, *Cell Calcium* **2004**, *35*, 427.
[20] R. S. Stephens, R. G. Bryant, *J. Biol. Chem.* **1976**, *251*, 403.
[21] P. S. Salmon, M.-C. Bellissent-Funel, G. J. Herdman, *J. Phys. Condens. Matter* **1990**, *2*, 4297.

[22] S.-H. Shin, M. B. Steffensen, T. D. W. Claridge, H. Bayley, *Angew. Chem.* **2007**, *119*, 7556; *Angew. Chem. Int. Ed.* **2007**, *46*, 7412.
[23] E. A. Richard, C. Miller, *Science* **1990**, *247*, 1208.
[24] V. M. Krishnamurthy, V. Semetey, P. J. Bracher, N. Shen, G. M. Whitesides, *J. Am. Chem. Soc.* **2007**, *129*, 1312.
[25] V. M. Krishnamurthy, L. A. Estroff, G. M. Whitesides in *Fragment-Based Approaches in Drug Discovery* (Eds.: W. Jahnke, D. A. Erlanson), Wiley-VCH, Weinheim, **2006**, p. 11.
[26] M. I. Page, W. P. Jencks, *Proc. Natl. Acad. Sci. USA* **1971**, *68*, 1678.
[27] M. H. Mazor, C. F. Wong, J. A. McCammon, J. M. Deutch, G. Whitesides, *J. Phys. Chem.* **1990**, *94*, 3807.
[28] NIST Critically Selected Stability Constants of Metal Complexes: Version 8.0. http://www.nist.gov/srd/nist46.htm.
[29] G. Fantuzzi, P. Pengo, R. Gomila, P. Ballester, C. A. Hunter, L. Pasquato, P. Scrimin, *Chem. Commun.* **2003**, 1004.
[30] E. Moczydlowski in *Ion Channel Reconstitution* (Ed.: C. Miller), Plenum, New York, **1986**, p. 75.
[31] U. Lindström, *Chem. Rev.* **2002**, *102*, 2751.
[32] A. J. Boersma, B. L. Feringa, G. Roelfes, *Angew. Chem.* **2009**, *121*, 3396; *Angew. Chem. Int. Ed.* **2009**, *48*, 3346.
[33] A. J. Boersma, J. E. Klijn, B. L. Feringa, G. Roelfes, *J. Am. Chem. Soc.* **2008**, *130*, 11783.
[34] H. Bayley, P. S. Cremer, *Nature* **2001**, *413*, 226.

